Article

A New Methodology to Evaluate High Temperature Mechanical Properties of Thin-Walled Tubes Using Ring Tension Specimen and Its Validation with Conventional Tests

A. Syed and M.K. Samal *

Article

A New Methodology to Evaluate High Temperature Mechanical Properties of Thin-Walled Tubes Using Ring Tension Specimen and Its Validation with Conventional Tests

A. Syed [1] and M. K. Samal [1,2,*]

[1] Division of Engineering Sciences, Homi Bhabha National Institute (HBNI), Mumbai-400094, India; ather@barc.gov.in

[2] Reactor Safety Division, Bhabha Atomic Research Centre (BARC), Trombay, Mumbai-400085, India; mksamal@barc.gov.in

* Correspondence: mksamal@barc.gov.in; Tel.: +91-22-2559 3551; Fax: +91-22-2550 5151

Abstract

The process of evaluation of mechanical properties of thin-walled small diameter tubes is cumbersome, especially, when the material exhibits significant anisotropy in the mechanical properties. For Zircaloy fuel clad tubes, the mechanical properties in the transverse or hoop direction are very different when compared to those along the length direction. As the diameter of the tubes is small, it is difficult to carry out conventional tensile tests and hence, ring tension tests are widely used. However, the ring tension test usually suffers from several drawbacks, such as the effect of friction between the ring and the loading mandrel on the stress-strain data and the existence of multi-axial state of stress in the gauge region. In this work, the effects of friction and state of stress have been taken into account in a new methodology, where the original load-displacement data is corrected for these effects using a correlation, which in turn has been derived from results of prior finite element analysis. The results of the new methodology have been validated by comparing data with those of conventional tensile tests. The new correlation has been used to evaluate transverse mechanical properties of Zircaloy-4 fuel clad over a wide temperature range, i.e., from 25°C to 900°C. This correlation has been used successfully for the first time in literature to evaluate the mechanical properties of Zircaloy-4 at such a high temperature environment. The data presented in this work is useful for safety analysts involved in simulation of severe accident progression and the correlation can be used to evaluate high temperature properties of similar thin-walled tubular components in industry.

Keywords: ring tension test; thin walled tubes; mechanical property; tensile test; high temperature property; Zircaloy-4; fuel clad; high temperature test

1. Introduction

Thin-walled tubular components are widely used in industry, such as heat exchanger tubes, pipes in refrigeration and air conditioning systems, pipes in chemical process industry and fuel clad in nuclear industry. Due to the variations in the manufacturing process, the microstructure and the grain structure of the corresponding alloys are not usually equi-axed and hence, these exhibit significant anisotropy in the mechanical properties. For the nuclear fuel clad, Zirconium based alloys are used and due to their hexagonally-closed-pack crystal structure, the mechanical properties of these tubes are different along the length and hoop directions as shown in Figure 1. For use in design and safety analysis, the transverse or hoop mechanical properties are required and hence, it becomes imperative to develop suitable experimental techniques to correctly evaluate these data.
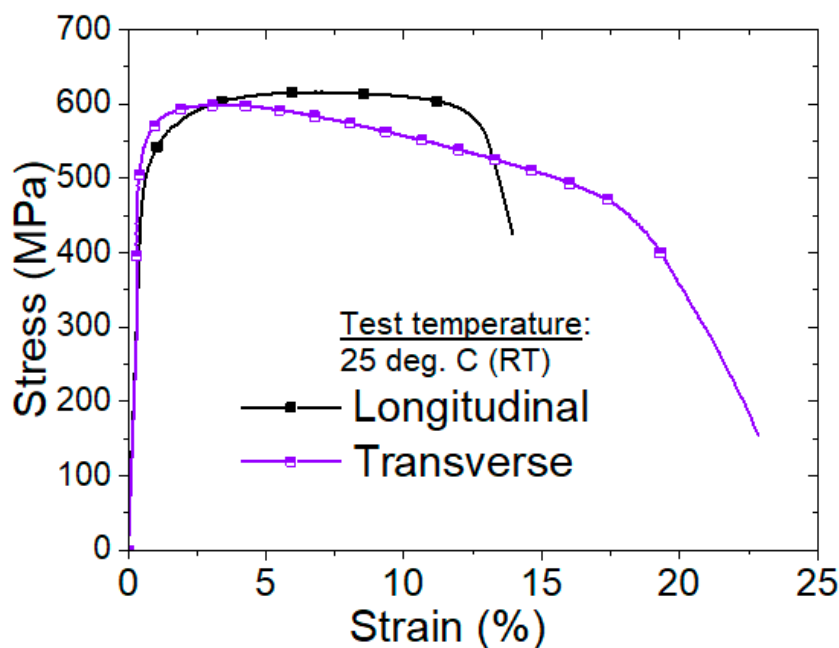
Figure 1. Engineering stress-strain data for longitudinal and transverse orientations of Zircaloy-4 thin-walled clad exhibiting significant anisotropy in the mechanical properties.

Arsene and Bai [1,2] were some of the few earlier pioneers, who had developed an approach for measuring the transverse properties of tubular components using a ring type test. Saikaly et al. [3] used both the ring expansion tests and standard tensile tests (using flat type specimens) to evaluate the mechanical properties of pipe-line steel. The results from both the tests were compared with each other. Wang et al. [4] and Bae et al. [5] also used similar ring specimens in their experiments.

Later, Arsène et al. [6] and Martín-Rengel et al. [7] used the similar type of ring specimen to evaluate the mechanical properties of hydrided fuel cladding in the hoop direction. Arsène et al. [6] also studied the effect of irradiation on change in mechanical properties of Zircaloy cladding tubes of pressurized water reactor and boiling-water reactors in both stress-relieved annealed and recrystallized annealed conditions. Kim et al. [8] studied the change in hoop strength and ductility of irradiated fuel cladding due to irradiation using ring tension tests.

Walsh and Adams [9] developed a ring test method, which uses four quadrants of loading mandrel instead of two D-shaped mandrels, in order to reduce the effect of friction between the specimen and the mandrel on the mechanical properties as obtained directly from the tests. Later, Nagase et al. [10] optimized the ring tensile test method to minimize the effect of friction and used the same test setup to evaluate the effect of hydrogen concentration in the matrix on the mechanical properties of Zircaloy cladding. Jiang and Wang [11] developed a conical wedge loaded ring expansion test, which is a modification of the conventional ring tension test.

The method of ring tension was extended to evaluate transverse properties of bigger size extruded tubes and pipes in Refs. [12–14]. This method is also used in Refs. [15–17] to evaluate the properties of different kinds of magnesium alloys, plasma-deposited metals and 3D-printed pipe respectively. The elastic and plastic material properties of additively manufactured alloys were evaluated using ring type specimens in Ref. [18]. The properties of recrystallized FeCrAl ODS (oxide dispersion strengthened) cladding tubes were evaluated using ring type specimen in Ref. [19] and these properties were correlated and with the corresponding evolution of microstructure and texture in the alloy. Similar studies were also reported in the works presented in Refs. [20–22].

Yoon et al. [23] have measured the elastic modulus of filament wound ring specimen using disk type of loading arrangement. The ring tension test-setup has been extensively modelled through finite element (FE) method in Refs. [24–28] in order to study the load-deformation behavior, state of

stress in the specimen and to evaluate the material stress-strain curve using an inverse identification technique [26,27]. Different states of stress during loading were created in the ring type specimen in Ref. [29] so that the failure locus of tubular components can be generated from these tests.

Later, several modifications to the ring tension test-setup, including various types of mandrel design and loading arrangements etc., have been reported in Refs. [30–32] and it was concluded that more accurate evaluation of the mechanical properties was possible when these new designs were used in the test. Recently, Hansen et al. [33] used a friction correction procedure in order to improve the accuracy while measuring the strength data in the ring tension test.

In summary, several studies are reported in literature, which discuss the methods to experimentally measure the transverse mechanical properties of tubular components. However, the issues of effect of friction between the specimen and the loading mandrel and presence of multi-axial state of stress in the deforming region of the ring specimens, are not easy to account for in a very generalized manner, as can be seen from a plethora of investigations reported in literature in recent years.

The objective of this work is to address the aspect of evaluation of transverse mechanical properties of Zircaloy-4 fuel clad of Indian PHWR (pressurized heavy water reactor) for a wide range of temperature environment (25-900°C) as these data are required for studying deformation of fuel clad during postulated severe accident scenarios. As the friction coefficient can vary depending upon the test temperature, this makes the task more challenging.

This paper is organized into six sections. After a presenting a brief description of the problem and review of relevant literature in Section 1, the material used in test, the specimen geometry and other test details are presented in Section 2. The results of finite element analysis of the ring tension test-setup have been discussed in Section 3, where the effect of friction, between the specimen and loading mandrel, on the load-displacement behavior has been extensively studied.

Based on the results of FE analysis, a new correlation for correction of load-displacement data has been derived and the details are presented in this section. Section 4 presents the results of ring tension tests conducted at different temperatures, which are subsequently corrected for the effect of friction. Some discussions regarding accuracy of these results and their comparison with conventional test data are presented in Section 5, followed by presentation of some of the important conclusions in Section-6.

2. Specimen Geometry, Loading Arrangement, Material Used in Experiment and Typical Test Data From Ring-Tension Test

In this work, the material of the ring specimen used in the test is Zircaloy-4 nuclear grade fuel clad, used in Indian PHWR. The details of chemical composition and microstructure of this material can be found in Ref. [34]. The fuel clad has the thickness 't' of 0.4 mm and the outer diameter 'D_o' is 15.2 mm. The geometry of the ring specimen as machined from the clad is shown in Fig. 2(a). The width 'w' of the ring specimen is taken as 3 mm. A typical image of the actual Zircaloy-4 ring specimen is shown in Figure 2(b), which has been machined in the length direction of the long fuel pin using wire EDM (electro-discharge machining) process. The fixture for loading the ring specimen is shown in Figure 2(c). The specimen is slipped into the two split D-shaped mandrels and the fixtures are connected to the loading strings of the test system.
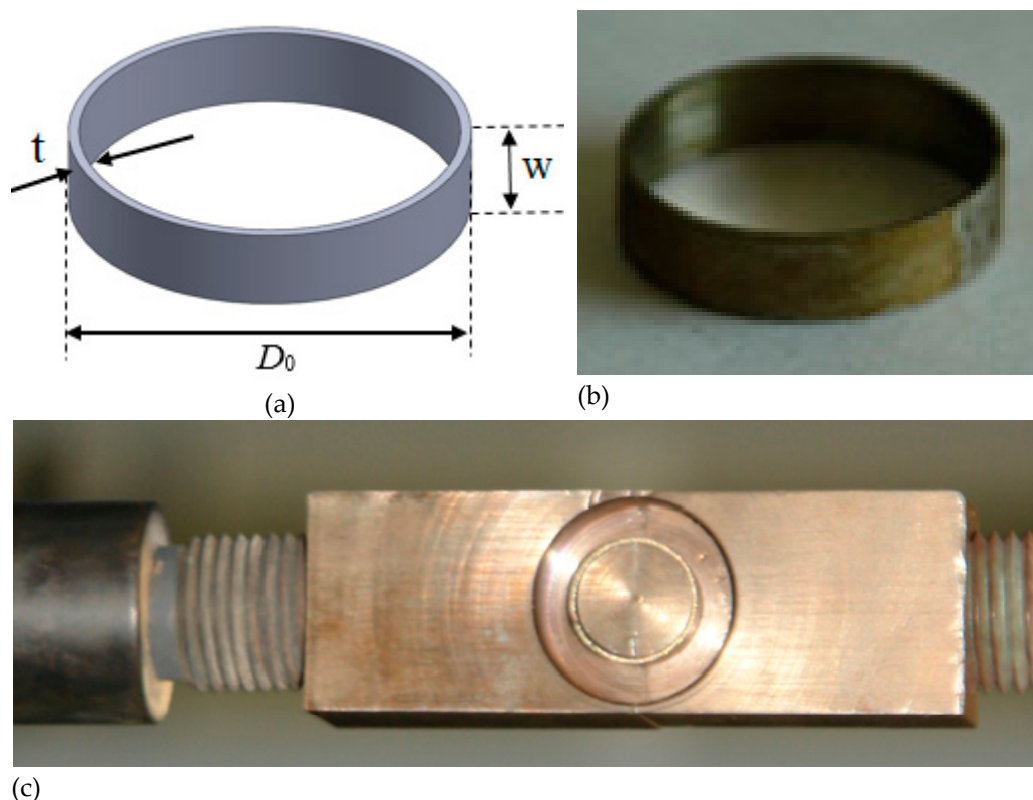
(a)

(b)

(c)

Figure 2. (a) Schematic geometry of the ring specimen machined from Zircaloy-4 fuel clad; (b) Picture of a typical ring specimen used in test; (c) Loading arrangement of ring specimens along with semi-cylindrical D-shaped split mandrels in a typical ring tension test setup.

Several ring tension tests have been conducted initially at two different temperatures, i.e., 25°C (room temperature condition) and 300°C. The load-displacement values, as obtained from the raw test data, have been converted to engineering stress-strain data using standard expressions. The engineering stress is obtained by dividing the load with twice the initial or original area of cross-section of the specimen as two gauge regions exist for the specimen, i.e., on either sides of the D-mandrels. Similarly, the engineering strain iscalculated by dividing the elongation with the gauge length, which is taken as 6 mm for this particular geometry of the specimen.

The details of estimation of gauge length for this particular geometry of ring specimen are discussed in Ref. [34]. Using the above procedure, the engineering stress-strain data has been evaluated from the tests and these are presented for the two test temperatures, i.e., 25°C and 300°C in Figure 3(a) and 3(b) respectively. The repeatability of test data has been shown in these figures by including results from atleast 3 tests for the similar test condition.

It may be noted that the strength properties, such as yield strength and ultimate tensile strength (UTS) are almost repeatable within an experimental scatter of $\pm 2\%$, whereas the scatter in ductility is slightly higher (of the order of 5 to 10%), when compared to that of scatter in strength data. It may be noted that these strength data contain the effect of friction between the specimen and the loading mandrel and hence, these data cannot be directly used as transverse mechanical properties of the material.

Hence, these data needs to be corrected for the above effect through a new correlation, the development of which shall be discussed in detail in the next section. Once the appropriate correlation to correct the effect of friction is developed in this work, the data as obtained directly from the ring tension tests shall be corrected and presented in the last section of the paper. In addition, the method shall be extended to the very high temperature range (i.e., 25°C to 900°C) and the corresponding corrected properties shall be presented for this alloy.
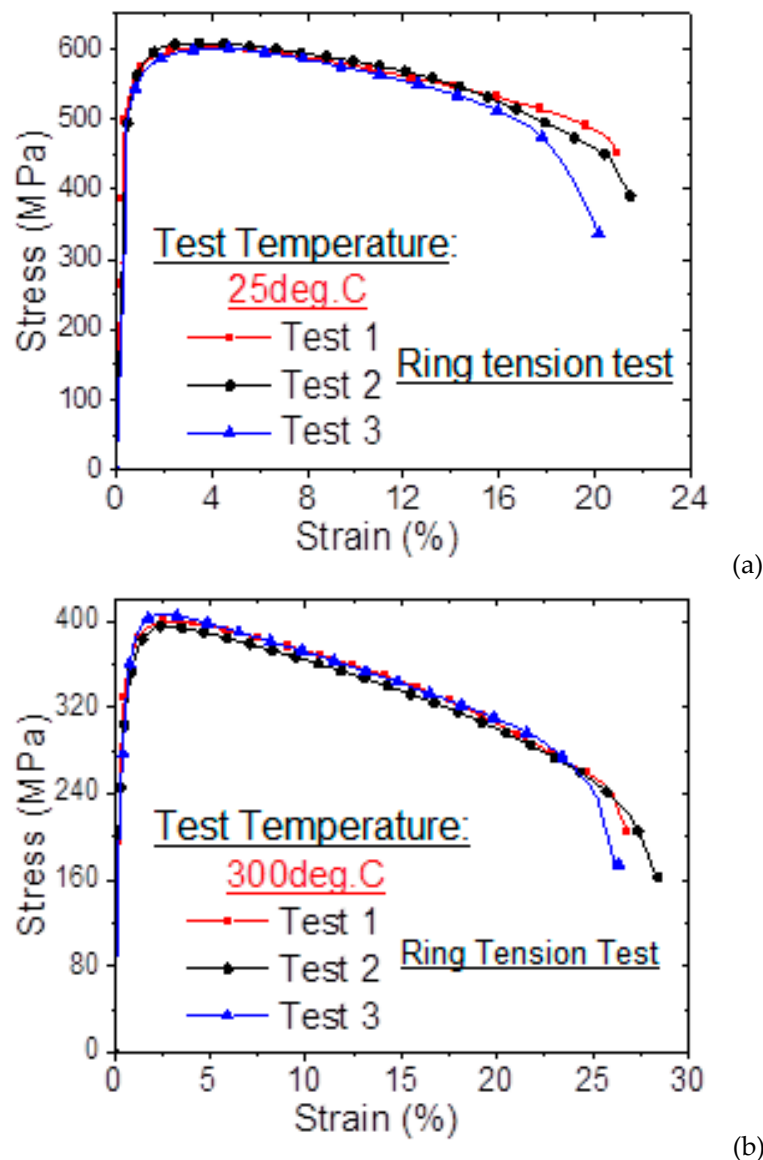
(a)

(b)

Figure 3. Repeatability of test as data obtained from ring tensile tests, which were carried out at two different temperatures. Test data at (a) 25°C (room temperature) and (b) 300°C.

3. Finite Element Analysis of Ring Tension Test Setup to Evaluate the Effect of Friction on Load-Displacement Data

In this section, the results of FE analysis of the ring tension test setup as shown in Figure 2(c) are presented for the two different test temperatures (i.e., 25°C and 600°C). The 3D finite element models of the specimen and the loading mandrel have been used in this work. 20-noded solid brick higher order elements have been used in the analysis. Elastic-plastic material model for the ring specimen has been used, whereas the mandrel is considered as elastic in nature. The details of material properties of the specimen and the mandrel used in the FE analysis are provided in Re. [34].

In addition, contact models have been included in the simulation. The effect of coefficient of friction, between the contacting surfaces (i.e., ring specimen inner diameter and D-mandrel outer diameter), has been taken into account. The coefficient of friction 'μ' varies depending upon the combination of materials at the contact surface and also it depends significantly on the temperature of the interface.

In this work, a vey generalized FE simulation has been carried out by varying by varying coefficient of friction 'μ' from 0 (no friction condition) to 1 (typical frictional value between metallic surfaces at very high temperature). As can be seen from the discussions later, this kind of parametric

study shall help us in generalizing and parameterizing the frictional effect so that the same can be taken care of easily while carrying out corrections in the load-displacement data as obtained directly from the ring tension tests. More details shall be provided later on this aspect.

Figure 4(a) shows the variation of load-displacement response of the ring specimen at room temperature (25ºC) for various magnitudes of coefficient of friction 'μ'. These values of 'μ' have been varied between 0 to 1 in order to cover a very wide range of friction conditions. It may be seen that the load carrying capacity of the ring specimen increases apparently due to increases value of friction, when a given displacement is imposed on the mandrel. Similar observation is also found in the results presented in Figure 4(b) for the case of 600ºC temperature environment. However, the load carrying capacity of the specimen at 600ºC is much lesser when compared to that of 25ºC as can be seen in Figure 4, which can be explained on the basis of lower material strength at elevated temperatures.
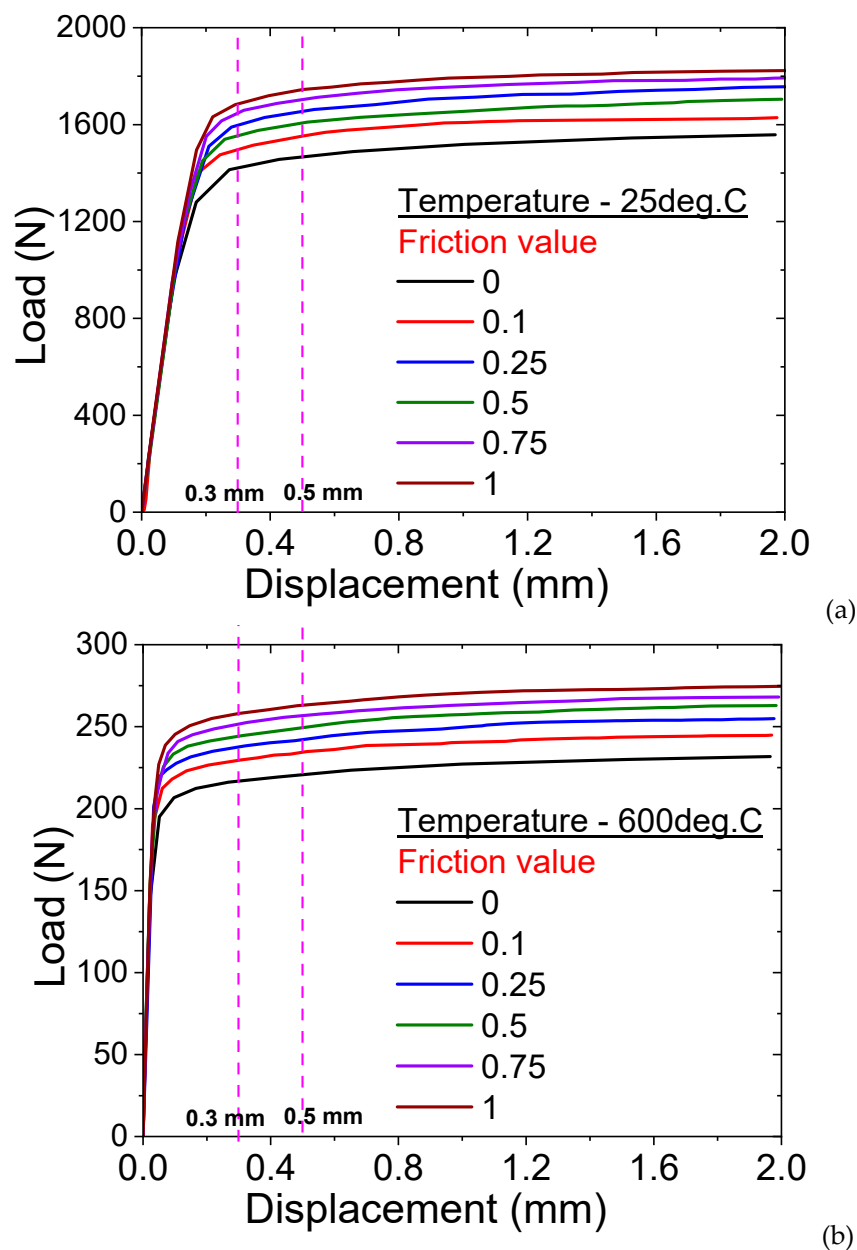

(a)

(b)

Figure 4. Load-displacement data as obtained from finite element simulation of ring tension test setup at two different temperatures assuming various magnitudes of coefficient of friction μ between the ring specimen and the mandrel. Variation of load-displacement curve at (a) 25ºC (room temperature condition) and (b) 600ºC for μ ranging from 0 to 1.

One consistent observation is that the apparent load carrying capacity always increases with respect to zero friction condition, when the coefficient of friction 'μ' is increased. On the other hand, though it may seem that, the apparent changes in absolute values of the load-carrying capacity of the specimen are less for 600°C loading case, when compared to that of 25°C loading case, the relative change in the load values are almost independent of test temperature, and this aspect shall be clearer later in the discussion.

For comparison of these two cases, the magnitudes of load at two different displacement values (i.e., 0.3 and 0,5 mm) have been taken and these are plotted as a function of coefficient of friction 'μ' in Figure 5(a) and 5(b) for the temperature of 25°C and 600°C respectively. It may be noted that the increase in load with 'μ' is almost same for both the temperatures and two values of applied displacements.
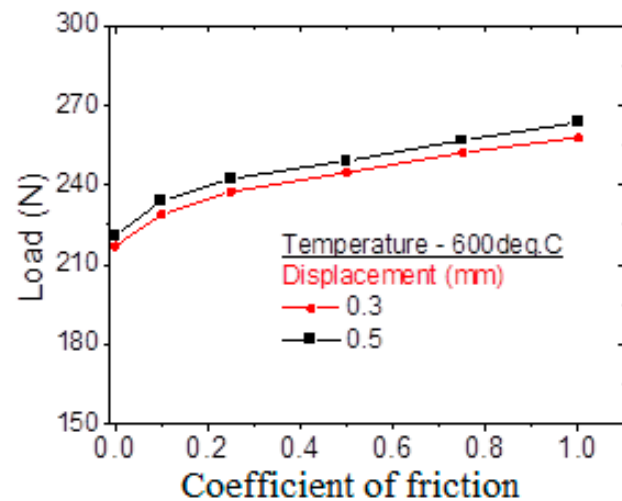
The nature of variation of load carrying capacity of the specimen with 'μ' is almost parallel to each other for the two displacements, and the load capacity of the specimen at 05 mm displacement is more compared to that for 0.3 displacement. The trend is similar for the case of 600°C temperature environment, except that the load magnitudes are relatively lower.

These data are normalized further with respect to the corresponding load values of 'μ=0' (i.e., frictionless) case and presented in Figure 6 for all the four combinations, i.e., 2 temperature and 2 displacement values. It can be observed from Figure 6 that the normalized load factor (also called normalization factor) is only dependent on the coefficient of friction 'μ' between the specimen and the mandrel.

The effects of temperature and loading magnitudes are in-built into the factor and hence, this is very generalized factor, which can be used effectively to correct the load-displacement data as obtained from the ring tension test in order to account for the effect of friction as well as the multiaxial state of stress in the specimen. This aspect shall be discussed later in detail where the validity of this correlation (i.e., between the normalization factor and coefficient of friction) shall be tested by comparing the corrected data of ring tensile specimens with those obtained from the conventional tests.
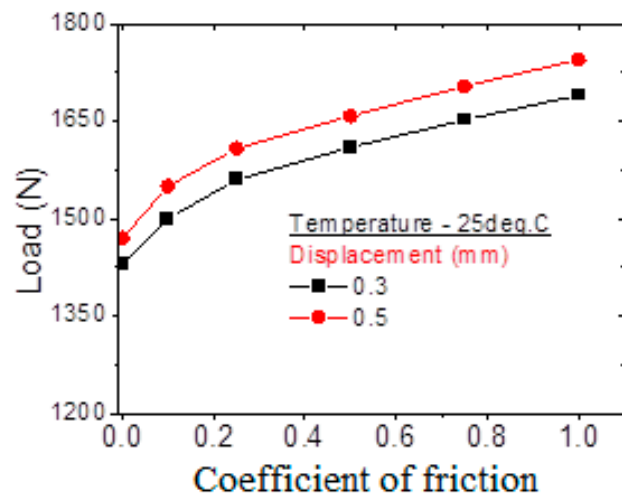
(a)

(b)

Figure 5. Variation of load carrying capacity of the ring specimen as a function of coefficient of friction for two different values of applied displacement loading and two different temperatures. Data at (a) 25°C (room temperature) and (b) 600°C.
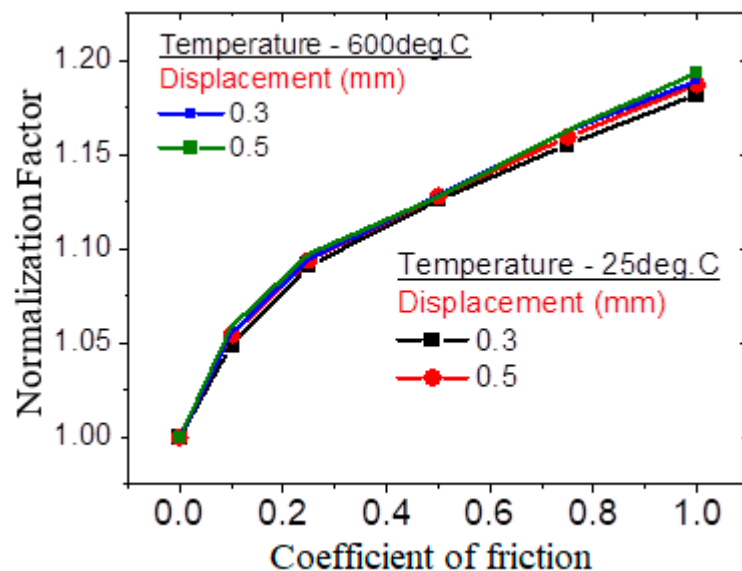

Figure 6. Variation of normalization factor with coefficient of friction showing its independence from temperature and the applied loading conditions.

4. Results

The variation of normalization factor with coefficient of friction 'μ' as presented in Figure 6 is the key result from this work, which has been used later to evaluate the friction-independent material stress-strain data and mechanical properties of Zircaloy-4 fuel clad of Indian PHWR. In order to use this correlation, one needs information regarding the friction coefficient between the Zircaloy-4 ring specimen and the steel mandrel. At room temperature (25°C), this value is estimated as 0.1.

It can be easily understood when one compares the load-displacements results of FE simulation (obtained with parametric variation of 'μ') with the actual experimental data as obtained from the ring tensile tests at the same temperature. This aspect was investigated in detail in an earlier publication by the authors and the specific details regarding this technique can be found in Ref. [34]. However, for same of completeness of discussion, it stated that the coefficient of friction 'μ' is identified by comparing the load-displacement data as obtained from FE simulation with the experimental data.

The corresponding load-displacement data of FE simulation with 'μ=0.1' is compared with the ring tension test data at 25°C in Figure 7(a). Similarly, the data from FE simulation with 'μ=0.6' is compared with the ring tension test data at 600°C in Figure 7(b). One may observe the satisfactory comparison of load-displacement data of FE simulation and experiment for both the temperature conditions. Hence, these two values of 'μ' are taken to be the magnitudes of coefficient of friction between Zircaloy-4 ring specimen and D-shaped steel mandrel at 25°C and 600°C respectively. These data points are plotted in Figure 7(c) and a trend line is fitted for both interpolation and extrapolation of values of 'μ' at other temperatures. These data along with correlation presented in Figure 6 has been used later in order to correct the load-displacement data of the ring tension tests at different temperatures and hence, to evaluate the mechanical properties of Zircaloy-4 fuel clad.
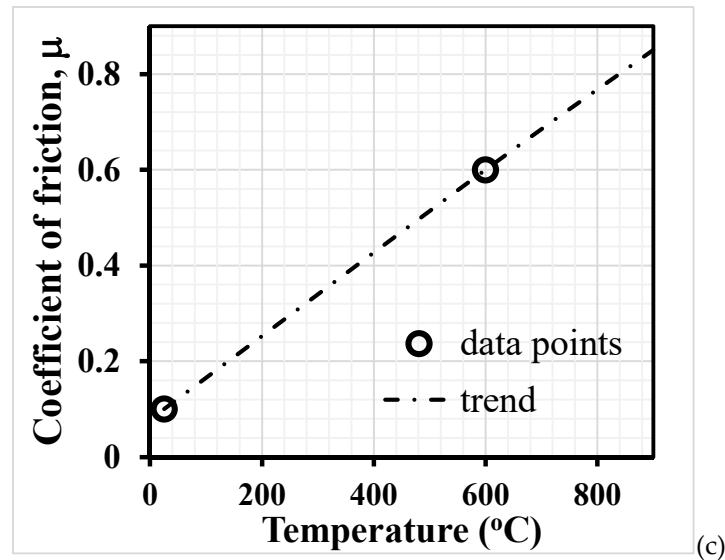

(a)

(b)

(c)
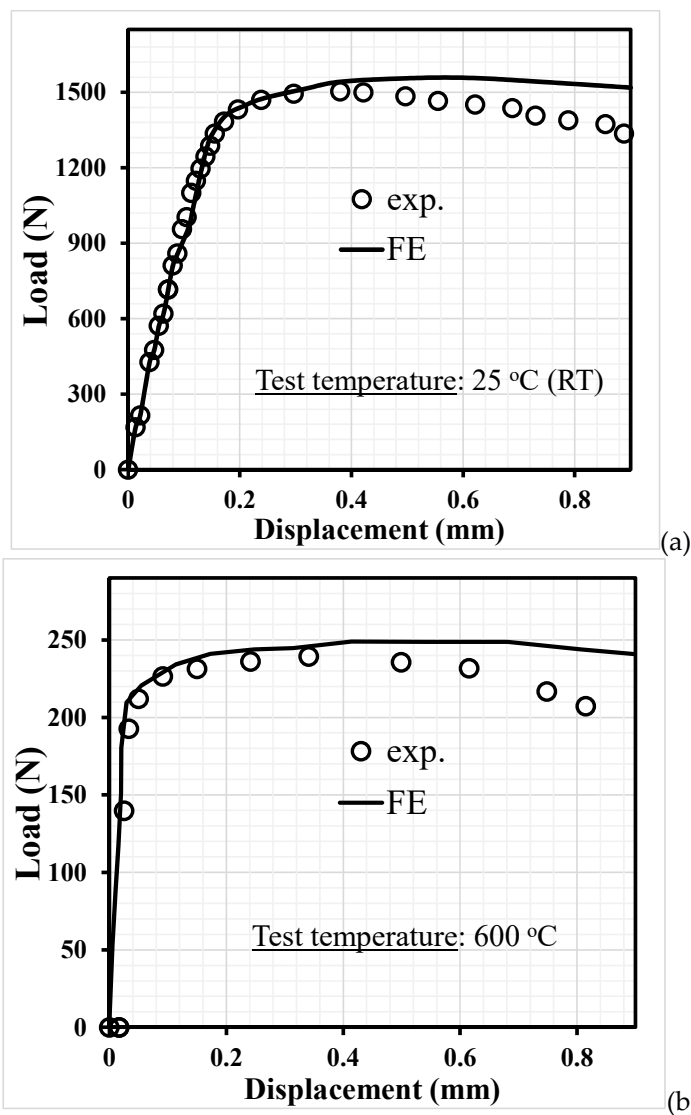
Figure 7. (a) Comparison of load-displacement data as obtained from finite element analysis of the ring tension specimen for (a) μ=0.1 at 25°C (room temperature); (b) μ=0.6 at 600°C, with corresponding experimental data; (c) Variation of coefficient of friction between Zircaloy-4 ring specimen and steel mandrel as a function of temperature.

5. Discussion

In order to validate the correlation derived in earlier section and presented in Figure 6, the corrected data from ring tension tests have been compared with conventional test data at two different temperatures (i.e., 25°C and 600°C) in Figure 8. The load-displacement data after correction has been converted to engineering stress-strain data and these are presented in Figure 8(a) for temperature of 25°C and in Figure 8(b) for temperature of 600°C.

It can be observed that the raw ring tensile data is on the higher side, when compared with the data of conventional test. This is due to the effect of friction and multiaxial state of stress as discussed earlier. However, after incorporating the correction, the stress-strain data obtained from the ring tension tests match closely with those of conventional test data. This observation seems to hold true for both the temperature cases as presented in Figs. 8(a) and 8(b) respectively.
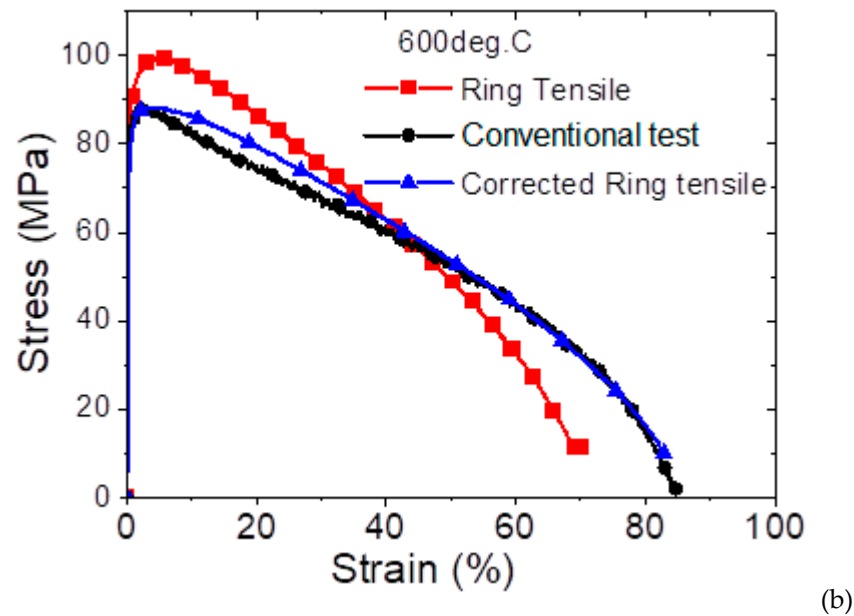

(a)

(b)
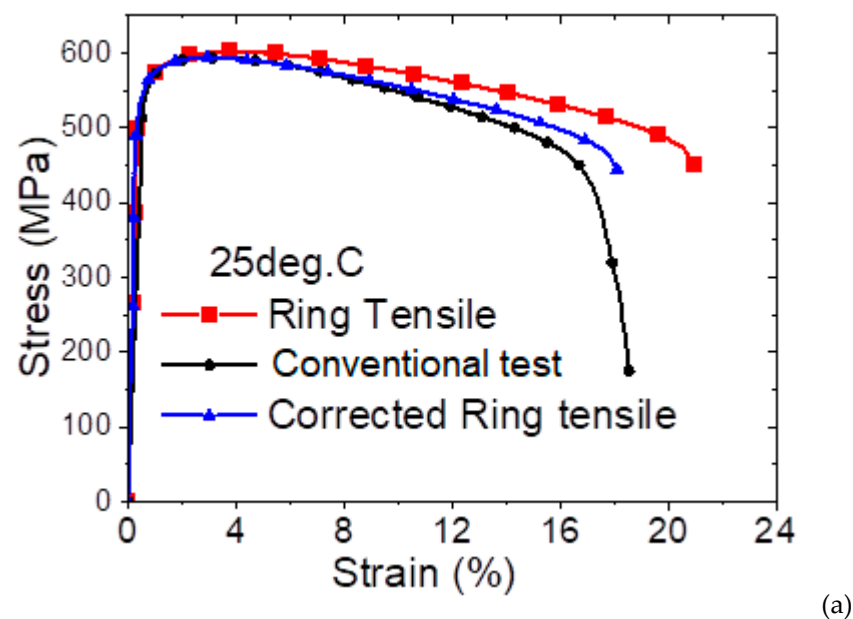
Figure 8. Comparison of stress-strain data as obtained from testing of ring tension specimens with the corrected data and those of conventional tests at two different test temperatures. Data at (a) 25°C and (b) 600°C.

The same procedure has been followed in order to evaluate the transverse mechanical properties of Zircaloy-4 fuel clad from corrected ring tension test data at different test temperatures ranging from 25°C to 900°C. The results are presented in Figs. 9 and 10 respectively. Figure 9 shows the corrected engineering stress-strain curves of Zircaloy-4 fuel clad in the above-mentioned temperature range. The mechanical properties, such as yield stress (YS), ultimate tensile strength (UTS) and ductility values, have been evaluated from this data and these are plotted at different temperatures in Figure 10 along with the statistical scatter bounds.

As can be seen from the above data, the strength properties (i.e., YS and UTS) decrease almost monotonically till the temperature of 650°C. After this temperature, the decrease in strength, is relatively slower, when compared to that found in the range of 25°C-650°C. On the other hand, the ductility increases monotonically till the temperature of 650°C and decreases with temperature when the temperature exceeds this value. This may be explained on the basis of change in microstructure and phase type in this alloy. The rate of increase of ductility is also higher in the temperature range of 400°C to 650°C. A thorough microstructural investigation is required in order to explain these changes more elaborately and this is a scope of future research for us. Nevertheless, these data are very useful to the engineers associated with the design and structural integrity analysis of nuclear fuel clad, especially, if one wants to simulate the progressive clad deformation during severe postulated severe accident scenarios, where very high temperature conditions are encountered routinely.
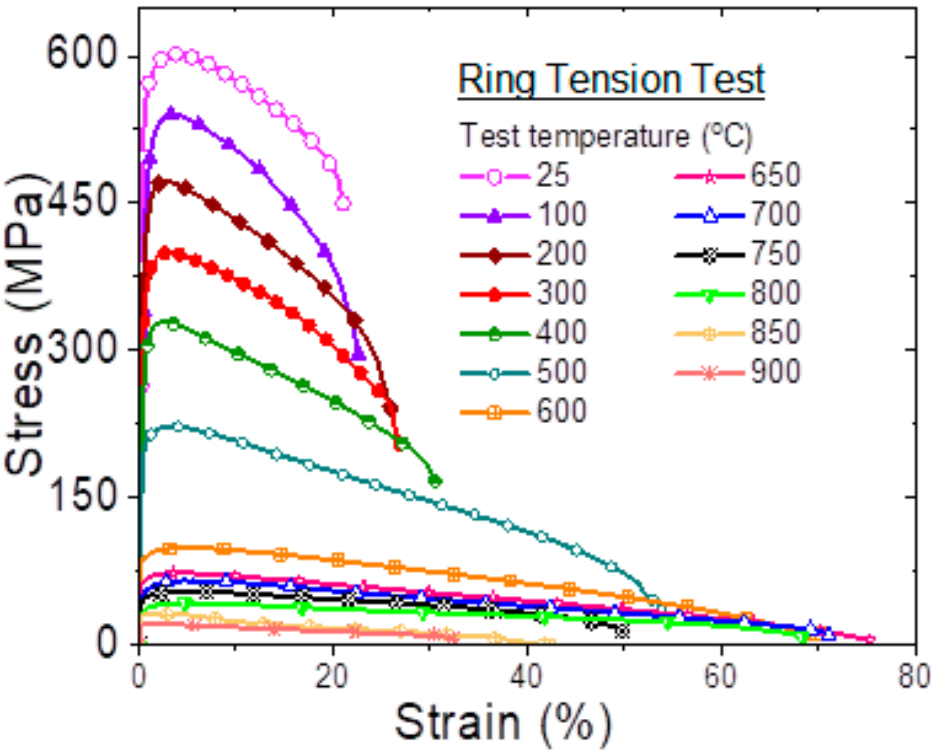
Figure 9. Corrected stress-strain data for transverse orientation of Zircaloy-4 fuel clad at different test temperatures ranging from 25°C (room temperature) to 900°C using the new correlation developed in this work.
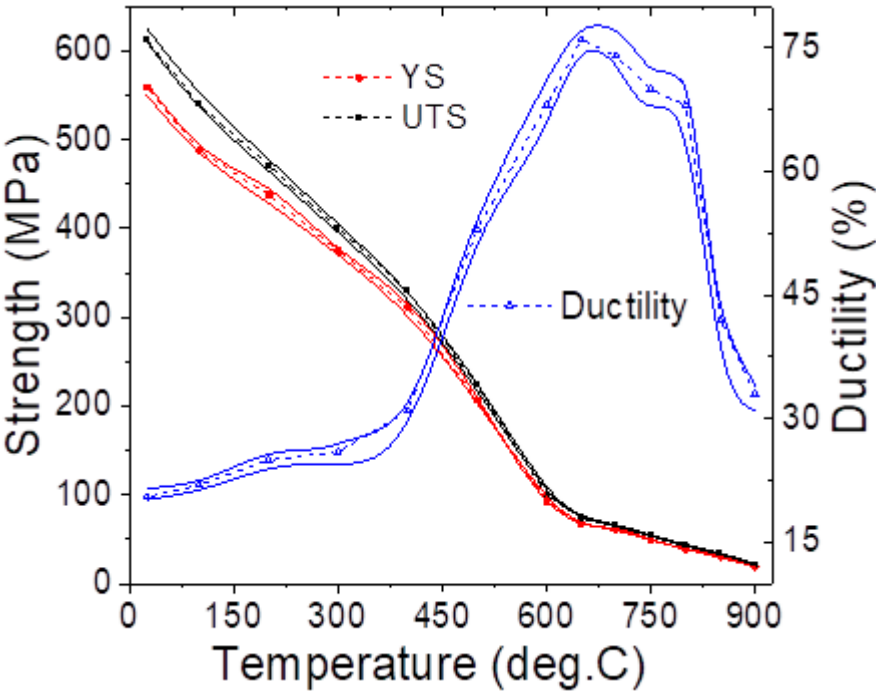

Figure 10. Variation of transverse orientation mechanical properties, such as yield stress, UTS, and ductility (along with the statistical scatter band) of Zircaloy-4 fuel clad at different test temperatures ranging from 25°C (room temperature) to 900°C.

6. Conclusions

In this work, ring tension tests have been carried out using specimens machined from the Zircaloy-4 fuel clad of Indian PHWR. Due to the effect of friction on load-displacement data and the

existence of multiaxial state of stress in the specimen, it is not straight forward to use this raw test data to evaluate the required mechanical properties. In order to overcome this issue, a new correlation has been developed, which has been used subsequently to evaluate the mechanical properties of Zircaloy-4 fuel clad in the temperature range of 25-900°C. The following conclusions can be derived from this work.

- The load carrying capacity of the ring specimen is dependent on the coefficient of friction between the ring specimen and the loading mandrel. As can be seen from results of FE analysis, the apparent load carrying capacity of the specimen increases with increasing value of 'μ'. As friction dissipates energy, more energy is needed to be given to the system in order to induce similar level of plastic deformation in the specimen. This explains the phenomenon of increase of load with 'μ'.

- The relative change in load magnitudes, i.e., when the load is normalized with the corresponding load values for the frictionless case, is found to be independent of temperature and level of loading.

- The variation of normalized load as a function of 'μ' may be specific to the material and geometry combination s encountered in the ring tensile tests. The above correlation has been found to predict the mechanical properties of Zircaloy-4 satisfactorily as it compares well with conventional test data.

- The correlation has been used to evaluate the mechanical properties of Zircaloy-4 fuel clad over a wide temperature range of 25-900°C. The change in strength values with temperature is monotonic in nature, whereas for the case of ductility, this data initially increase till 650°C, and decreases slightly afterwards, which may be explained based on the microstructural and corresponding phase changes in this alloy at higher temperatures. Similar observations are also found for similar type of Zirconium based alloys in literature. However, this requires detailed further investigation.

- The data presented in this work shall be useful to designer and safety analysts concerned with study of high temperature deformation behavior of fuel clad during postulated severe accident scenarios.

References

1. Arsene, S.; Bai, J. A new approach to measuring transverse properties of structural tubing by a ring test. ASTM Journal of Testing and Evaluation, 24, 1996, pp. 386–391. https://doi.org/10.1520/JTE11461J
2. Arsène S., Bai J. A new approach to measuring transverse properties of structural tubing by a ring test - experimental investigation. ASTM Journal of Testing and Evaluation, 26, 1998, 26–30. https://doi.org/10.1520/JTE11966J

3. Saikaly E.; Bailey D.; Collins E. Comparison of ring expansion vs. flat tensile testing for determining line-pipe yield strength. In Proceedings of the 1996 1st International Pipeline Conference, Calgary, AB, Canada, 9–13 June 1996; pp. 209–213.

4. Wang H., Bouchard R., Eagleson R., Martin P., Tyson W. Ring hoop tension test (RHTT): a test for transverse tensile properties of tubular materials. Journal of Testing and Evaluation, 30, 2002, 382. https://doi.org/10.1520/JTE12328J

5. Bae B.-K., Cho S.-K., Seok C.-S. A study on ring tensile specimens. Materials Science and Engineering: A, 483–484, 2008, pp. 248-250. https://doi.org/10.1016/j.msea.2006.10.203.

6. Arsène S., Bai J., Bompard P. Hydride embrittlement and irradiation effects on the hoop mechanical properties of pressurized water reactor and boiling-water reactor Zircaloy cladding tubes: part III. Mechanical behavior of hydride in stress-relieved annealed and recrystallized condition. Metallurgical and Materials Transactions A 34, 2003, 579–588. https://doi.org/10.1007/s11661-003-0093-1

7. Martín-Rengel M.A., Gómez Sánchez F.J., Ruiz-Hervías J., Caballero L., Valiente A. Revisiting the method to obtain the mechanical properties of hydrided fuel cladding in the hoop direction. Journal of Nuclear Materials, 429, 2012, pp. 276–283. https://doi.org/10.1016/j.jnucmat.2012.06.003

8. Kim S.K., Bang J.G., Kim D.H., Lim I.S., Yang Y.S., Song K.W., Kim D.S. Hoop strength and ductility evaluation of irradiated fuel cladding. Nuclear Engineering and Design 239, 2009, pp. 254–260. https://doi.org/10.1016/j.nucengdes.2008.10.024

9. Walsh E.J., Adams D.O. Development and evaluation of the quadrant ring test method. Proc Soc Exp Mech Inc 65, 2008, pp. 319–326. https://doi.org/10.1007/s11340-007-9089-x

10. Nagase F., Sugiyama T., Fuketa T. Optimized ring tensile test method and hydrogen effect on mechanical properties of Zircaloy cladding in hoop direction. Journal of Nuclear Science and Technology, 46, 2009, pp. 545–552. https://doi.org/10.1080/18811248.2007.9711560

11. Jiang H., Wang J.A.J. Development of cone-wedge-ring-expansion test to evaluate the tensile hoop properties of nuclear fuel cladding. Progress in Nuclear Energy, 108, 2018, pp. 372–380.

12. Dick C.P., Korkolis Y.P. Assessment of anisotropy of extruded tubes by ring hoop tension test. Procedia Engineering, 81, 2014, pp. 2261-2266. https://doi.org/10.1016/j.proeng.2014.10.318.

13. Barsoum I.; Ali K. Development of a method to determine the transverse stress-strain behavior of pipes. Procedia Engineering, 130, 2015, pp. 1319–1326.

14. Barsoum I., Ali K.F.A. A procedure to determine the tangential true stress-strain behavior of pipes. International Journal of Pressure Vessels and Piping, 128, 2015, pp. 59-68. https://doi.org/10.1016/j.ijpvp.2014.11.002.

15. Jiang L., Jonas J.J., Boyle K., Martin P. Deformation behavior of two Mg alloys during ring hoop tension testing. Materials Science and Engineering A, 492 (1–2), 2008, pp. 68–73.

16. Mehan R.L., Jackson M.R., Rairden J.R., Carter W.T. The use of a ring tensile test to evaluate plasma-deposited metals. Journal of Material Science, 22, 1987, pp. 4476–4483. https://doi.org/10.1007/BF01132050

17. Travica M.; Mitrovic N.; Petrovic A.; Trajkovic I.; Milosevic M.; Sedmak A.; Berto F. Experimental evaluation of hoop stress–strain state of 3D-printed pipe ring tensile specimens. Metals, 12, 2022, 1560. https://doi.org/10.3390/met12101560

18. Rouse J.P., Simonelli M., Hyde C.J. On the use of small ring testing for the characterization of elastic and yield material property variation in additively manufactured materials. Additive Manufacturing, 36, 2020, 101589.

19. Aghamiri S.M.S., Sowa T., Ukai S., Oono N., Sakamoto K., Yamashita S. Microstructure and texture evolution and ring-tensile properties of recrystallized FeCrAl ODS cladding tubes. Materials Science and Engineering A, 771, 2020, 138636. https://doi.org/10.1016/j.msea.2019.138636.

20. Frolov A.S., Fedotov I.V., Gurovich B.A. Evaluation of the true-strength characteristics for isotropic materials using ring tensile test. Nuclear Engineering and Technology, 53(7), 2021, pp. 2323-2333. https://doi.org/10.1016/j.net.2021.01.033.

21. Hansen R.S., Kamerman D.W., Petersen P.G., Cappia F. Evaluation of the ring tension test (RTT) for robust determination of material strengths, International Journal of Solids and Structures, 282, 2023, 112471. https://doi.org/10.1016/j.ijsolstr.2023.112471

22. EL-Bagory T.; Alarifi I.; Younan Y. Prediction of mechanical properties for curved dumbbell-shaped specimen at different orientation angles of ring hoop tension test. Advanced Engineering Materials, 21, 2019, 1900191.

23. Yoon S.H., Cho W.M., Kim C.G. Measurement of modulus in filament wound ring specimen using split disk test. Experimental Techniques, 21, 1997, pp. 25–28. https://doi.org/10.1111/j.1747-1567.1997.tb00488.x

24. He Z., Yuan S., Zha W., Liang Y. Force and deformation analysis of tube ring specimen during hoop tension test. Jinshu Xuebao/ Acta Metallurgica Sinica, 44, 2008, pp. 423–427

25. Calaf-Chica J., Martínez-Peña J., Díez P.M.B., Calzada M.P. Ring hoop tension test for yield strength estimation: Numerical analysis for a novel correlation method and applicability for mechanical testing of tubes and pipes. Mechanics of Materials, 169, 2022, 104295. https://doi.org/10.1016/j.mechmat.2022.104295.

26. Samal M.K., Balakrishnan K.S., Parashar J., Tiwari G.P. Investigation of deformation behavior of ring-tensile specimens machined from pressure tubes of Indian PHWR. Transactions of Indian Institute of Metals, 67, 2014, pp. 167–176. https://doi.org/10.1007/s12666-013-0314-2

27. Ktari Z., Carlos L.; Pedro A.; Ali K. Mechanical design of ring tensile specimen via surrogate modelling for inverse material parameter identification. Mechanics of Materials, 153, 2021, 103673. https://doi.org/10.1016/j.mechmat.2020.103673

28. Dick C.P., Korkolis Y.P. Mechanics and full-field deformation study of the ring hoop tension test. International Journal of Solids and Structures, 51(18), 2014, pp. 3042-3057. https://doi.org/10.1016/j.ijsolstr.2014.04.023

29. Al-Khaled M.A., Barsoum I. New ring specimen geometries for determining the failure locus of tubular components. Transactions of ASME Journal of Pressure Vessel Technology, 140, 2018, 403831. https://doi.org/10.1115/1.4038311

30. Ali K., Ktari Z., Carlos L. New mandrel design for ring hoop tensile testing. Experimental techniques, 45, 2021, pp. 769-787.

31. Kazakeviciute J., Rouse J.P., De Focatiis D.S., Hyde C.J. The development of a novel technique for small ring specimen tensile testing. Theoretical and Applied Fracture Mechanics, 99, 2019, pp. 131–139.

32. Ktari Z., Khalfallah A. Design and validation of a new ring hoop plane strain test for characterizing the anisotropic plastic behavior of tubular materials. International Journal of Solids and Structures, 298, 2024, 112869. https://doi.org/10.1016/j.ijsolstr.2024.112869.

33. Hansen R.S., Kamerman D.W., Petersen P.G., Cappia F., Liu J., Jiao Y. Friction corrections to improve accuracy of cladding strength measurements from the ring tension test. Proceedings of the 2023 Water Reactor Fuel Performance Meeting, Springer Nature Singapore, pp. 317-329. https://doi.org/10.1007/978-981-99-7157-2_33

34. Samal M.K.; Syed A.; Chattopadhyay J.; Vaswani S.; Ram A.M. Compendium of Indian NPP material properties generated by RSD, BARC. Volume VII- Version 1: Zirconium alloys, BARC External Report No. BARC/2022/E/001, April 2022.